Presented at the 11th Annual CMAS Conference, Chapel Hill, NC, October 15-17, 2012

INFLUENCE OF MODEL GRID RESOLUTION ON NO_2 VERTICAL COLUMN DENSITIES OVER EAST ASIA

Kazuyo Yamaji*
Japan Agency for Marine-Earth Science and Technology, Yokohama, Japan

Hitoshi Irie
Chiba University, Chiba, Japan

Jun-ichi Kurokawa
Asia Center for Air Pollution Research, Niigata, Japan

Toshimasa Ohara
National Institute for Environmental Studies, Tsukuba, Japan

1. INTRODUCTION

NO_x (NO + NO_2) emitted from fossil-fuel combustion, biomass burning, soil microbial processes, and lightning plays important roles in the troposphere such as ozone production, aerosol formation and atmospheric composition through feedback on OH_x (OH + HO_2 + RO_2). As compared with relatively long-lived species, however, the modeled reproducibility by chemical transport models (CTMs) would be inferior. Especially for industrial regions, e.g. eastern China which is the largest emission area in East Asia, CTMs tended to underestimate NO_2 vertical column densities (VCDs) from satellite retrievals (e.g., van Noije et al., 2006; Uno et al., 2007). They discussed this discrepancy from viewpoints of both retrievals and CTMs and emission inventories, however the exact reason remained unclear.

It is known that species subject to non-linear sources or sinks are susceptible to biases in coarse-resolution CTMs. Wild et al. (2006) indicated that the export of short-lived precursors such as NOx by convection is overestimated at coarse resolution. Valin et al. (2011) concluded that resolution in the range of 4–12 km is sufficient to accurately model nonlinear effects in the NO_2 loss rate.

In this study, we evaluate influence of model horizontal grid resolutions on NO_2 vertical column densities in June and December 2007 over East Asia by using the Community Multiscale Air Quality modeling system (CMAQ) (Byun and Schere, 2006) with updated and elaborated regional emission inventory in Asia (REAS) (Ohara et al., 2007).

**Corresponding author:* Kazuyo Yamaji, Research Institute for Global Change, Japan Agency for Marine-Earth Science and Technology, 3173-25 Showa-machi, Kanazawa-ku, Yokohama 236-0001 Japan; e-mail: kazuyo@jamstec.go.jp

2. MODEL DESCRIPTION

The modeling system employed in this study was CMAQ ver.4.7.1 driven by the Weather Research and Forecasting (WRF) ver.3.3 (Skamarock and Klemp, 2008). The WRF simulation used NCEP Final Analysis (ds083.2) for the year 2007. Detailed model setups are shown in Table 1.

The vertical layers consist of 37 sigma-pressure coordinated layers from the surface to 50 hPa with the first layer height being around 20 m. Fig. 1 shows modeling domains with NO_2 emissions. The horizontal resolutions and the numbers of grid cells are 80, 40, 20, and 10 km and 95 × 75, 110 × 88, 184 × 132, and 292 × 182 for D1, D2, D3, and D4, respectively.

Anthropogenic emissions over East Asia were re-gridded from updated REAS sets for monthly at 0.25° × 0.25°. Biomass burning and biogenic emissions are used from RETRO (http://retro.enes.org) and MEGANv2 (http://acd.ucar.edu/~guenther), respectively. Fig. 1 shows NO_2 emissions in June 2007 for D1, D2, D3, and D4, respectively. NO_2 emissions in June 2007 were divided for central east China (CEC, latitude and longitude as 28°-43° and 110°-123°) as 1.1 kmoles s^{-1} in all domains.

Table1 Model setup or WRF and CMAQ

WRF		CMAQ	
microphysics	Thompson	advection	PPM
PBL physics	ACM2	vertical diffusion	ACM2(inline)
longwave	RRTM	gas-chemistry	SAPRC99
shortwave	Dudhia	solver	EBI
		aerosol-chemistry	AERO5
		cloud module	cloud_acm_ae5

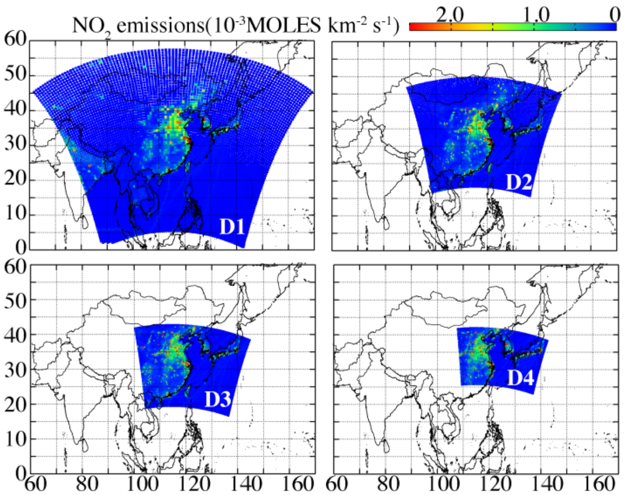

Fig. 1 NO_2 emissions in June 2007

3. RESULTS AND DISCUSSION

3.1 Comparisons of CMAQ NO_2 VCDs and satellite retrievals

Simulated NO_2 VCDs in June and December 2007 are compared with three tropospheric NO_2 retrievals from three different satellite sensors, global ozone monitoring experiment–2 (GOME-2), scanning Imaging absorption spectrometer for atmospheric chartography (SCIAMACHY), and OMI (ozone monitoring instrument) with the same basic algorithm (DOMINO products for OMI and TM4NO2A products for SCIAMACHY and GOME-2) (Irie et al., 2012). As for the comparisons with GOME-2, SCIAMACHY, and OMI passing over the equator at about 9:30 LT, 10:00 LT, and 13:45 LT, in this study, CMAQ NO_2 VCDs at 9:00 CST (Chinese Standard Time), 10:00 CST, and 14:00 CST was used, respectively.

Fig 2 shows monthly averaged NO_2 VCDs from satellite sensors, GOME-2 and OMI and simulations with different spatial resolutions, 80km (D1), 40km (D2), 20km (D3), and 10km (D4). This model system using CMAQ v4.7.1 with updated REAS had a good performance for simulating tropospheric NO_2 VCDs over East Asia. Generally, this model system could capture well the spatial distributions and concentration levels the retrieved NO_2 VCDs even by using the coarsest resolution (D1).

As for the afternoon case in June, the finer scale simulations, e.g. D3 and D4, produced in detail horizontal distribution patterns of NO_2 VCDs over the North China Plain with comparing to the coarse resolution (D1) having monotonic NO_2 VCDs distributions, which were more close to the GOME-2 retrieval. On the other hand, CMAQ tended to overestimate the retrieved NO_2 VCDs at the high emission areas in the North China Plain, especially at Shanghigh. The overestimation was enhanced in the finer resolutions. As for the morning case in December, NO_2 VCDs on progressing from D1 to D2, D3, and D4 were increased, but CMAQ NO_2 VCDs even by using D4 partially underestimated a little the retrieved NO_2 VCDs over North China Plain. Meanwhile, increased NO_2 VCDs due to the progression of the model resolution made the overestimation enhance over the ocean.

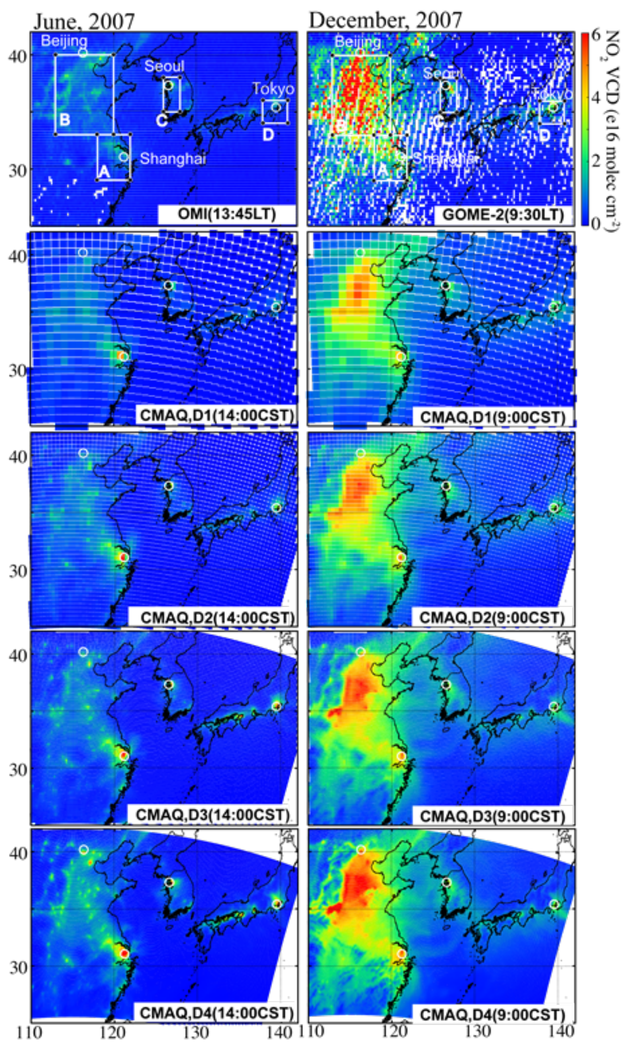

Fig. 2 Monthly averaged NO_2 VCDs in the afternoon in June 2007 (left column) and the morning in June 2007 (right column). Satellite retrievals from OMI at 13:45 LT (left) and GOME-2 at 13:45 LT (right) in the first line. CMAQ NO_2 VCDs at 14:00 CST (left) and 9:00 CST (right) by using D1, D2, D3, and D4 in the lower lines. The diagnostic regions (A, B, C, and D) enclosed with white lines were used in the present studies.

3.2 Biases between satellite retrievals and CMAQ NO_2 VCDs in the different horizontal resolutions

Fig. 3 shows relationships between satellite retrievals by using monthly averages for each 1° ×1° grid of GOME-2, SCIAMACHY, and OMI and CMAQ NO_2 VCDs within all, A, B, C, and D regions shown in Fig. 2. These correlations were reasonable, and that meant that the distributions of satellite retrievals and CMAQ NO_2 VCDs were quite similar. The progressing from D1 to D2, D3, and D4 for four diagnostic regions (A, B, C, and D) resulted as increases in NO_2 VCDs excepting a few grids. In June, regardless of timings or sensors in the observations, CMAQ NO_2 VCDs are closer to satellite retrievals than those in December, even in D1. Meanwhile, the progress from D1 to D2, D3, and D4 enhanced the overestimation of NO_2 VCDs in this model.

In December, on the other hand, CMAQ NO_2 VCDs were lower than satellite retrievals over relatively-polluted regions, all diagnostic regions and higher than those over the other area. Especially in the afternoon, CMAQ NO_2 VCDs agreed well with OMI NO_2 VCDs. As for the morning, however, CMAQ NO_2 VCDs underestimated the satellite retrievals, GOME-2 and SCIA over polluted regions.

Table 2 summarizes the monthly biases (%) between CMAQ NO_2 VCDs and satellite retrievals for regional averages. The progress of modeled special resolutions, from D1 to D2, D3, and D4 made increases in the monthly and regional averaged CMAQ NO_2 VCDs, but it was not necessarily make improvements the biases between CMAQ NO_2 VCDs and satellite retrievals.

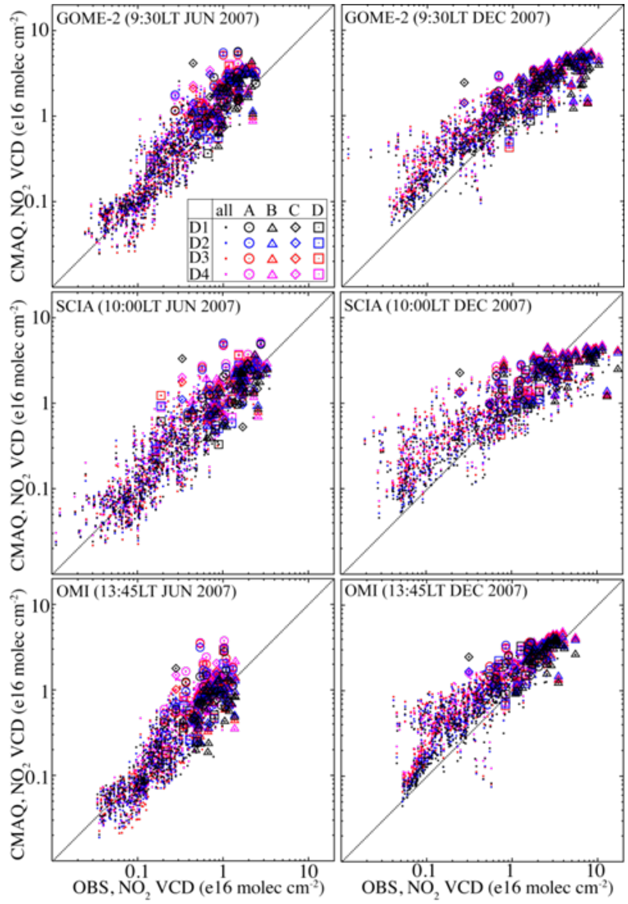

Fig. 3 Scatter plots between monthly NO_2 VCDs from satellite retrievals, GOME-2 (upper), SCIAMACHY (middle), and OMI (lower) and CMAQ by using averaged concentrations in a 1° ×1° grid within all, A, B, C, and D regions shown in Fig. 2. Only areas covered by D4 were used. The all, A, B, C, and D regions includes 574-579, 16-15, 42, 6, and 6 grids, respectively.

Table 2 Biases* between satellite retrievals and CMAQ NO_2 VCDs

	all				A				B				C				D			
	D1	D2	D3	D4	D1	D2	D3	D4	D1	D2	D3	D4	D1	D2	D3	D4	D1	D2	D3	D4
									JUN 2007											
GOME-2	47	63	69	78	77	121	119	130	47	65	73	80	94	80	103	121	54	60	117	99
SCIA	-47	-40	-37	-32	27	60	65	70	-2	12	19	30	-4	-9	5	20	3	15	56	46
OMI	2	12	18	38	53	102	121	136	-9	1	4	38	18	18	38	76	1	20	64	66
									DEC 2007											
GOME-2	-6	5	12	17	26	39	51	58	-32	-23	-21	-18	34	36	44	46	0	-1	1	2
SCIA	-36	-29	-23	-20	0	10	19	24	-53	-48	-46	-43	8	10	17	18	-3	-4	-2	-1
OMI	39	55	67	76	49	66	78	87	9	21	26	32	84	90	102	107	58	57	63	66

*Biase(%)=(CMAQ NO_2 VCDs - satellite NO_2 VCDs) / satellite NO_2 VCDs *100, using monthly and regional averages for the diagnostic regions (A, B, C, and D shown in Fig. 2).

Table 3 Simulated vertical column densities of NOx, NOy, and NOz (N 10^{15} molec. cm^{2})

	A				B				C				D			
	D1	D2	D3	D4	D1	D2	D3	D4	D1	D2	D3	D4	D1	D2	D3	D4
JUN 2007 (9:00 CST)																
NOx	4.4	5.2	5.2	5.5	3.9	4.2	4.5	4.7	2.8	3.0	3.4	3.6	1.8	2.1	3.0	2.7
NOy	7.0	7.7	8.0	7.9	8.8	9.0	9.3	8.8	5.2	5.3	5.8	5.3	3.0	3.2	4.2	3.2
NOz	2.6	2.5	2.8	2.5	4.9	4.8	4.8	4.2	2.4	2.3	2.4	1.8	1.2	1.1	1.2	0.5
JUN 2007 (13:00 CST)																
NOx	4.0	4.4	4.8	5.2	5.6	6.2	6.3	6.8	2.5	2.7	2.9	3.0	2.1	2.3	2.4	2.4
NOy	6.6	7.0	7.8	7.8	9.9	10.5	10.8	10.8	4.9	5.0	5.3	4.8	3.3	3.3	3.6	3.0
NOz	2.7	2.6	2.9	2.6	4.3	4.4	4.6	4.0	2.4	2.3	2.4	1.8	1.2	1.1	1.2	0.5
DEC 2007 (9:00 CST)																
NOx	5.5	6.2	6.9	7.4	8.0	8.9	9.2	10.1	3.4	3.8	4.2	4.3	2.9	3.2	3.5	3.6
NOy	12.7	13.3	14.7	15.7	15.9	16.7	16.6	18.2	8.0	8.5	8.7	8.6	4.6	4.9	5.3	5.4
NOz	7.2	7.1	7.7	8.3	7.9	7.8	7.4	8.1	4.6	4.7	4.5	4.4	1.7	1.7	1.8	1.8
DEC 2007 (13:00 CST)																
NOx	5.7	6.5	7.2	7.6	8.0	8.9	9.2	10.1	3.3	3.7	4.1	4.3	2.9	3.3	3.6	3.7
NOy	13.1	13.7	15.1	16.1	15.5	16.3	16.2	17.7	7.5	7.8	8.1	8.2	4.7	5.0	5.4	5.6
NOz	7.4	7.3	7.9	8.4	7.5	7.4	7.0	7.6	4.2	4.1	3.9	3.9	1.7	1.7	1.9	1.9

NOy=NO+NO2+NO3+HNO3+HONO+2(N2O5)+PAN+ANO3(i+j), NOz=NOy-NOx, using monthly and regional averages for the diagnostic regions (A, B, C, and D shown in Fig. 2).

3.3 Simulated vertical column densities of NOx, NOy, and NOz in different horizontal resolutions

Table 3 summarizes the monthly and regional averaged CMAQ NOx, NOy, and NOz VCDs over four diagnostic regions (A, B, C, and D). Generally, both of NOx and NOy VCDs were increased with progressing from D1 to D2, D3, and D4, although a little NOy VCDs decrease was shown in D4 of C and D in the afternoon in June. The largest increments in the change from D_x to D_{x+1} appeared in the morning were 18% at A (from D1 to D2), 12% at B (from D1 to D2), and 13% at C (from D2 to D3) and 42% at D without linear increments in the sequence, D1-D2-D3-D4, and that were affected by both of *in-situ* non-linear chemistry and its transport. Additionally, the clear convergence in NOx and NOy VCDs changes was not found in the sequence, D1-D2-D3-D4.

NOz VCDs changes due to horizontal resolution changes from D1 to D2, D3, and D4 were not simple for each region, season, and time. Mostly NOz VCDs over Chinese diagnostic regions, A and B, clearly decreased with spatial distribution changes from D1 to D2, and then NOz VCDs in D4 increased in December and decreased in June. In Jun, NOz VCDs over A, C, and D have same changes, up-down-up, in the sequences, D1-D2-D3-D4. In December, NOz VCDs decrease over C and increase over D from D1 and D2 to D3 and D4. NOz VCDs changes in the progressing from D1 to D2, D3, and D4 were complicate. Although those reasons were unclear, that seemed to be caused by *in-situ* non-linear chemistries of both themselves and more short lived nitrogen oxides and their transports.

4. SUMMARY

We have used a regional CTM, CMAQ, at a sequence of four horizontal resolutions, 80, 40, 20, and 10 km (D1, D2, D3, and D4) in June and December 2007 to investigate influence of horizontal resolution at nitrogen oxides VCDs.

Monthly averaged CMAQ NO_2 VCDs comprehensively compared with three tropospheric NO_2 retrievals from three different satellite sensors, GOME-2, SCIAMACHY, and OMI. CMAQ could capture well the retrieved NO_2 VCDs even by using the coarsest resolution (D1). This model system using CMAQ v4.7.1 with updated REAS had a good performance for simulating tropospheric NO_2 VCDs over East Asia.

CMAQ NO_2 VCDs generally increased due to the progressing from D1 to D2, D3, and D4, and that made biases between CMAQ and satellite retrievals both larger and smaller. The finer horizontal resolutions not necessarily show better agreement with the satellite retrievals in this study. CMAQ NO_y VCDs were mostly increased in finer horizontal resolutions.

NOz VCDs changes due to horizontal resolution changes were not simple for each region, season, and time, caused by *in-situ* non-linear chemistries of both themselves and more short-lived nitrogen oxides and their transports.

5. ACKNOWLEDGEMENTS

This work is partially supported by the Global Environment Research Fund (S-7) of the Ministry of the Environment, Japan and the support program for young and women researchers of University of Tokyo.

6. REFERENCES

Byun, D. and K. L. Schere. 2006: Review of the governing equations, computational algorithms, and other components of the models-3 community multiscale air quality (CMAQ) modeling system. *Appl. Mech. Rev.* **59**, 51-76.

Irie, H., K. F. Boersma, Y. Kanaya, H. Takashima, X. Pan, and Z. F. Wang, First quantitative bias estimates for tropospheric NO2 columns retrieved from SCIAMACHY, OMI, and GOME-2 using a common standard, *Atmos. Meas. Tech. Discuss.* **5**, 3953-3971, 2012.

Ohara, T., H. Akimoto, J. Kurokawa, N. Horii, K. Yamaji, X. Yan, and T. Hayasaka, 2007: An Asian emission inventory of anthropogenic emission sources for the period 1980–2020. *Atmos. Chem. Phys.* **7**, 4419-4444.

Skamarock, W. C. and J. B. Klemp. 2008: A time-split nonhydrostatic atmospheric model for weather research and forecasting applications. *J. Comput. Phys.* **227**, 3465-3485.

Uno, I., Y. J. He, T. Ohara, K. Yamaji, J. Kurokawa, M. Katayama, Z. Wang, K. Noguchi, S. Hayashida, A. Richter, and J. P. Burrows, 2007: Systematic analysis of interannual and seasonal variations of model-simulated tropospheric NO2 in Asia and comparison with GOME-satellite data. *Atmos. Chem. Phys.* **7**, 1671-1681.

Valin, L. C., A. R. Russell, R. C. Hudman, and R. C. Cohen, 2011: Effects of model resolution on the interpretation of satellite NO_2 observations. *Atmos. Chem. Phys.*, **11**, 11647-11655.

van Noiji, T. P. C., Eskes, H. J., Dentener, F. J., et al., 2006: Multimodel ensemble simulations of tropospheric NO_2 compared with GOME retrievals for the year 2000, *Atmos. Chem. Phys.* **6**, 2943–2979.